Journal of Sound and Vibration (1999) **227**(5), 1003–1017
Article No. jsvi.1999.2393, available online at http://www.idealibrary.com on IDEAL®

ON THE SCATTERING OF SOUND BY A RECTILINEAR VORTEX

M. S. Howe

Boston University, College of Engineering, 110 *Cummington Street, Boston, MA* 02215, *U.S.A.*

(*Received* 30 *October* 1998, *and in final form* 3 *May* 1999)

A re-examination is made of the two-dimensional interaction of a plane, time-harmonic sound wave with a rectilinear vortex of small core diameter at low Mach number. Sakov [1] and Ford and Smith [2] have independently resolved the "infinite forward scatter" paradox encountered in earlier applications of the Born approximation to this problem. The first order scattered field (Born approximation) has nulls in the forward and back scattering directions, but the interaction of the wave with non-acoustically compact components of the vortex velocity field causes wavefront distortion, and the phase of the incident wave to undergo a significant variation across a parabolic domain whose axis extends along the direction of forward scatter from the vortex core. The transmitted wave crests of the incident wave become concave and convex, respectively, on opposite sides of the axis of the parabola, and focusing and defocusing of wave energy produces corresponding increases and decreases in wave amplitude. Wave front curvature decreases with increasing distance from the vortex core, with the result that the wave amplitude and phase are asymptotically equal to the respective values they would have attained in the absence of the vortex. The transverse acoustic dipole generated by translational motion of the vortex at the incident wave acoustic particle velocity, and the interaction of the incident wave with acoustically compact components of the vortex velocity field, are responsible for a system of cylindrically spreading, scattered waves outside the parabolic domain.

1. INTRODUCTION

It has been conjectured that the Born (or first order scattering) approximation leads to an ill-posed problem when applied to the two-dimensional interaction of sound with a rectilinear vortex of non-zero total circulation [3–7]. Direct numerical simulations for an incident plane wave at low Mach numbers [6, 9] yield estimates of the scattered sound that are finite in all radiation directions and in good qualitative agreement with experiment [10–12], whereas scattering theory apparently predicts infinitely intense "forward" scattered sound. The same approximation gives finite scattered sound levels when the vorticity distribution has zero net circulation [1, 13–17].

O'Shea [3] correctly attributed the difficulty to the long range convection (or *refraction*) of sound by the mean velocity field of the vortex, which decays slowly like $1/r$, where r is distance from the vortex axis. Scattering theory imposes

0022-460X/99/451003 + 15 $30.00/0

a radiation condition that, at large distances, scattered waves must radiate away from the vortex axis. However, when the interaction region is very extensive, some of the scattered waves will themselves radiate through the vortex core, and great care must therefore be exercised to extract this behavior from a solution expressed in terms of cylindrical harmonics centered on the core. This difficulty was resolved by Sakov [1] and by Ford and Smith [2]. The correct behavior of the scattered sound in the near field can be ensured by imposing *causality* rather than an outgoing wave condition. Careful asymptotic evaluation of the corresponding integral representation supplies a scattered field that is finite in all directions and, in particular, predicts a null in the forward direction, in accordance with predictions for scattering by acoustically compact (low Mach number) turbulence eddies [18–20]. Sakov [1] showed that the scattered sound had different representations depending on whether the field point was within or outside a parabolic domain whose axis extends from the vortex in the direction of forward scatter. Outside the parabola, scattering is dominated by waves that have *constant strength* along rectilinear rays radiating out from the vortex; in addition there exist much weaker, cylindrically spreading waves of the type normally associated with an outgoing wavefield. Within the parabola both of these components are of comparable magnitudes and cancel in the direction of forward scatter.

The length scale of the vortex velocity (the inverse of its fractional rate of change with distance) increases with distance from the vortex. Ultimately, at sufficiently large distances, the incident wave will therefore propagate according to *ray theory* [21–23], and a complete description of the vortex–wave interaction should arguably quantify the roles of the refracted incident wave and the cylindrically scattered waves. Ford and Smith [2] used the method of matched asymptotic expansions, and their solution is actually valid to a higher order than the usual approximation of first order scattering theory. Detailed predictions are in broad agreement with the numerical results of Colonius *et al.* [6]. In both of these investigations the importance of long-range "refraction" by the weakly decaying rotating flow induced by the vortex is fully emphasized, although no attempt is made to exhibit it explicitly by incorporating the refractive component of scattering into a "renormalized" incident wave whose evolution as it propagates across the vortex flow can then be examined.

The present paper has two objectives. First, the scattering problem is recast using the equation of vortex sound. This isolates unambiguously a term describing scattering by the vortex, which appears as a dipole source, and that accounting for refraction by the mean flow, which occurs in the wave operator applied to the acoustic variable. A zeroth order approximation to the refracted wave can be written down from this equation by inspection. This approximation fails in the parabolic region bounding the forward scattering direction. Second, the zeroth order approximation is corrected by consideration of the full Born approximation. The full solution can be represented as a combination of a transmitted incident wave, modified by refraction by the moving medium, and cylindrically scattered waves. The zeroth order solution develops a phase shift when the incident wave passes through the vortex core, with a "phase jump" along the forward scattered ray from the vortex. This phase jump is eliminated in the full Born approximation, which predicts a smooth transition across the parabolic domain, such that the phase shift relative to the undisturbed incident wave vanishes along the forward scattered ray. The parabola expands to fill all the space at large distances to the rear of the vortex, and the transmitted incident wave ultimately *relaxes* to its undisturbed form.

The scattering problem is formulated in section 2. The zeroth order solution and the full Born approximation are discussed in section 3. The solution is interpreted in section 4 in terms of refracted and cylindrically propagating scattered waves.

2. THE GOVERNING EQUATIONS

A small amplitude, plane sound wave of radian frequency ω propagates in the positive direction of the x-axis of the rectangular co-ordinate system (x, y, z) in a uniform, homogeneous fluid of density ρ_0 and sound speed c_0. The wave impinges on a line (or "point") vortex of circulation Γ lying along the z-axis, as illustrated schematically in Figure 1. It is required to calculate the secondary sound waves produced during the interaction.

Thermal and viscous dissipation will be ignored, and the fluid motion regarded as homentropic. The exact, non-linear equation of vortex sound theory may then be cast in the form [4, 20]

$$\left(\frac{D}{Dt}\left(\frac{1}{c^2}\frac{D}{Dt}\right) - \frac{1}{\rho}\,\nabla\cdot(\rho\,\nabla)\right)B = \frac{1}{\rho}\operatorname{div}(\rho\boldsymbol{\omega}\wedge\mathbf{v}), \tag{1}$$

where $\mathbf{v}$ is the fluid velocity, $\boldsymbol{\omega} = \operatorname{curl}\mathbf{v}$ the vorticity, and $\rho \equiv \rho(\mathbf{x}, t)$, $c \equiv c(\mathbf{x}, t)$ are, respectively, the fluid density and sound speed, both of which depend on position and the time t. B is the *stagnation enthalpy* which, for homentropic flow, is given in

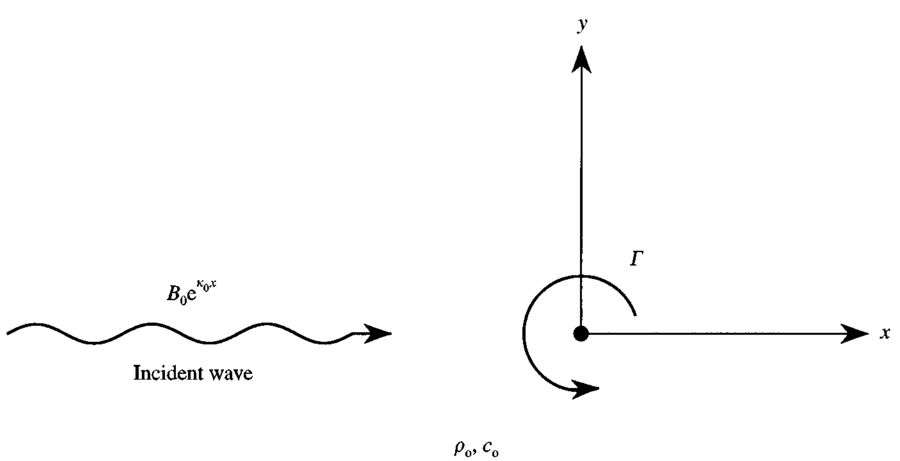

Figure 1. Time harmonic plane wave incident on a line vortex of strength Γ. The z-axis is directed out of the plane of the paper.

terms of the pressure p, density $\rho \equiv \rho(p)$ and velocity by

$$B = \int \frac{\mathrm{d}p}{\rho} + \frac{1}{2} v^2. \tag{2}$$

In those regions where $\boldsymbol{\omega} = 0$, the motion can be expressed in terms of a velocity potential φ, say, and Bernoulli's equation implies that $B = -\partial\varphi/\partial t$. Thus, we can take $B = 0$ in the absence of sound, when the fluid is in a state of steady circulatory flow induced by the vortex.

The linearized equation describing small amplitude fluctuations about this steady state produced by the impinging sound is deduced from equation (1) by replacing all variable coefficients in the wave operator on the left hand side by their respective mean values. The characteristic Mach number M of the mean flow is assumed to be sufficiently small that variations in the mean density and sound speed (which are of order M^2 relative to their undisturbed values) can be neglected, and we therefore set $c = c_0$, and $\rho = \rho_0$ on the left-hand side of equation (1). Although this condition on M is violated in the immediate neighborhood of the vortex, where the mean velocity is indefinitely large, the solution obtained for this case can be interpreted as an "elementary solution" from which the solution of the general problem involving distributed vorticity $\boldsymbol{\omega}$ with finite-induced velocity $\mathbf{v}$ can be derived by convolution. We shall not discuss this extension, but it may also be noted that, when the wavelength of the incident wave is large compared with the vortex core, the precise details of the core vorticity can have no material influence on the properties of the scattered sound, even in the presence of a singular (but integrable) velocity at the core.

The Born approximation determines the scattered field correct to terms that are linear in both the incident wave amplitude and the amplitude of the scattering inhomogeneity. Consider time harmonic motion, and let the incident wave be

$$B_i = B_0 \mathrm{e}^{\mathrm{i}(\kappa_0 x - \omega t)}, \quad B_0 = \text{constant}, \tag{3}$$

where $\kappa_0 = \omega/c_0$ is the acoustic wavenumber and, without loss of generality, it may be assumed that $\omega > 0$. In the absence of this wave, the vortex is at rest and $B = 0$. Therefore, in equation (1) we can take

$$B = B_i + B_s, \quad \boldsymbol{\omega} = \Gamma \mathbf{k} \delta(x)\delta(y), \tag{4}$$

where B_s is the scattered field and $\mathbf{k}$ is a unit vector parallel to the vortex (the z-axis). Then, to first order in Γ equation (1) becomes

$$\left(\nabla^2 + \frac{2\mathrm{i}\kappa_0}{c_0} \nabla\Phi \cdot \nabla + \kappa_0^2 \right) B = -\frac{\partial}{\partial y}\left(\frac{\Gamma B_0}{c_0} \delta(x)\delta(y) \right), \tag{5}$$

where the exponential time factor $\mathrm{e}^{-\mathrm{i}\omega t}$ is here and henceforth suppressed.

In this equation, B_0/c_0 is the acoustic particle velocity of the incident wave (which is parallel to the x-axis) evaluated at the undisturbed position of the vortex, and Φ is the velocity potential of the mean velocity field of the vortex, which we take in the form

$$\Phi = \frac{-\Gamma \operatorname{sgn}(y)}{2}\left(H(x) - \frac{\operatorname{sgn}(x)}{\pi}\arctan\left|\frac{y}{x}\right|\right), \tag{6}$$

where $H(x)$ is the Heaviside step function ($=0$, 1 according as $x \lessgtr 0$). Because this term occurs in the wave operator its principal effect is to *refract* the incident sound, at least for $x < 0$ before the wave reaches the singularity at the vortex core.

In general, the velocity potential of the vortex is not single valued, but increases by $n\Gamma$ for a field point that traverses a path encircling the vortex n times in the anticlockwise direction [24], although the velocity is continuous. Our definition (6) restricts Φ to lie in the range $(-\frac{1}{2}\Gamma, +\frac{1}{2}\Gamma)$, with a discontinuity along a radial "cut" in the forward scattering direction ($x > 0$, $y = 0$). This is a convenient analytical prescription which, of course, does not imply that the scattered sound is discontinuous across the cut.

By substituting from the first of equation (4) into equation (5), and noting that $(\nabla^2 + \kappa_0^2)B_i = 0$, the equation determining the scattered field B_s in the Born approximation is found to be

$$(\nabla^2 + \kappa_0^2)B_s = -\frac{\partial}{\partial y}\left(\frac{\Gamma B_0}{c_0}\,\delta(x)\delta(y)\right) + \frac{2\kappa_0^2 B_0}{c_0}\,\frac{\partial \Phi}{\partial x}\,\mathrm{e}^{\mathrm{i}\kappa_0 x}. \tag{7}$$

The first term on the right is a dipole concentrated at the vortex core, arising from the induced translational motion of the vortex at the acoustic particle velocity of the incident wave. The second term is distributed over the whole of the flow, and includes components with length scales that are both large and small compared with the wavelength of the incident wave, and therefore accounts for both refraction and scattering of the sound.

3. SOLUTION OF THE SCATTERING PROBLEM

3.1. ZEROTH ORDER APPROXIMATION

A preliminary indication of the influence of the mean circulatory flow produced by the vortex is obtained by noting that, *correct to first order in*

$$\varepsilon = \frac{\kappa_0 \Gamma}{c_0}, \tag{8}$$

a solution of the *homogeneous* form of equation (5) (when the dipole source is discarded) can be cast in the form [4, 20, 25]

$$B = B_0 \mathrm{e}^{\mathrm{i}\kappa_0 (x - \Phi(\mathbf{x})/c_0)}. \tag{9}$$

This will be called the *zeroth order* approximation; it is uniformly valid in those regions where $M^2 \equiv |\nabla\Phi|^2/c_0^2 \ll 1$, and reduces to the incident wave (3) as $x \to -\infty$, where $\Phi(\mathbf{x}) \to 0$. However, because $\Phi(\mathbf{x})$ is discontinuous across $x > 0$, $y = 0$, the solution (9) is physically unacceptable in the vicinity of the forward scattering direction, across which it exhibits a *phase jump* equal to

$$-\frac{\kappa_0}{c_0}[\Phi(x, y)]_{y=-0}^{+0} = \frac{\kappa_0 \Gamma}{c_0} \equiv \varepsilon, \quad x > 0.$$

But this phase discontinuity gives an accurate representation of the dominant effect of the vortex on the sound: the phase of waves in the "upper" region $y > 0$ is advanced by the flow, and that of waves in the lower region ($y < 0$) is retarded. This is illustrated in Figure 2 for $\varepsilon = \pi$, which shows the evolution of successive "wave crests" (curvilinear lines of constant phase differing by 2π) defined by

$$\frac{x}{\lambda} + \frac{\varepsilon}{4\pi}\,\mathrm{sgn}(y)\left(H(x) - \frac{\mathrm{sgn}(x)}{\pi}\arctan\left|\frac{y}{x}\right|\right) = n, \quad n = 0, \pm 1, \pm 2, \dots, \qquad (10)$$

where $\lambda = 2\pi/\kappa_0$ is the wavelength of the incident sound.

Because of the phase jump across the forward scattering ray ($x > 0$, $y = 0$), wave crests in $y < 0$ are half a wavelength ahead of those in $y > 0$. Careful inspection of Figure 2 reveals a progressive and smooth distortion of wave fronts approaching the vortex (from $x < 0$) which eventually develops into a discontinuity as a front crosses the core of the vortex. The solution of the Born approximation equation (7), discussed in section 3.2, reveals the existence of a transition region (first identified by Sakov [1]) bounded by the parabola $x \approx (\kappa_0/\pi)y^2$ (the broken line curve in the figure), across which the upper and lower families of wave crests are smoothly joined.

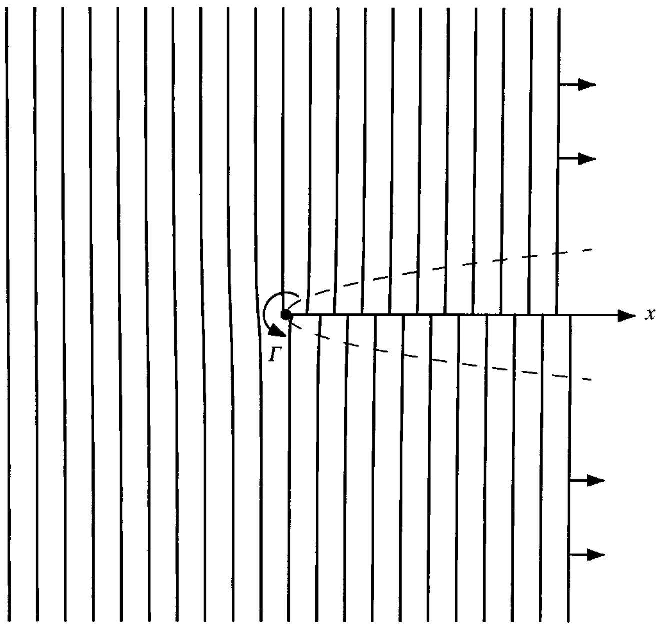

Figure 2. Wave crests defined by equation (10) for the zeroth order approximation (9) when $\varepsilon = \pi$. For $x > 0$ the waves in the lower region ($y < 0$) are approximately half a wavelength ahead of those in $y > 0$. The solution is strictly valid outside the broken-line parabola ($x \approx (\kappa_0/\pi)y^2$), within which the full solution of section 3.2 predicts a smooth transition between the upper and lower wave regions.

3.2. THE BORN APPROXIMATION

Let the total scattered sound be written

$$B_s = B_\Gamma + B_\Phi, \tag{11}$$

where B_Γ and B_Φ correspond, respectively, to the two source terms on the right of equation (7). Since $B = -(\mathrm{i}/4)H_0^{(1)}(\kappa_0 r)$, $r=\sqrt{x^2+y^2}$, is the solution with outgoing wave behavior of $(\nabla^2+\kappa_0^2)B = \delta(x)\delta(y)$ [20], where $H_0^{(1)}$ is a zero order Hankel function, it follows that the dipole component of the radiation, B_Γ, is given by

$$B_\Gamma = \frac{\mathrm{i}\Gamma B_0}{4c_0}\frac{\partial H_0^{(1)}(\kappa_0 r)}{\partial y} \sim \frac{-\kappa_0 \Gamma B_0}{c_0\sqrt{8\pi \mathrm{i}\kappa_0 r}}\frac{y}{r}\,\mathrm{e}^{\mathrm{i}\kappa_0 r}, \quad r=\sqrt{x^2+y^2}\to\infty. \tag{12}$$

This represents a cylindrically spreading disturbance centered on the vortex.

The component B_Φ produced by the distributed source on the right of equation (7) is conveniently determined by the method of double Fourier transforms, defined according to the reciprocal formulae

$$\hat{\mathscr{F}}(k,l) = \frac{1}{(2\pi)^2}\iint_{-\infty}^{\infty}\mathscr{F}(x,y)\mathrm{e}^{-\mathrm{i}(kx+ly)}\,\mathrm{d}x\,\mathrm{d}y,$$

$$\mathscr{F}(x,y) = \iint_{-\infty}^{\infty}\hat{\mathscr{F}}(k,l)\mathrm{e}^{\mathrm{i}(kx+ly)}\,\mathrm{d}k\,\mathrm{d}l.$$

The Fourier transform of the source is

$$\frac{\mathrm{i}\kappa_0^2\Gamma B_0 l}{2\pi^2 c_0(l^2+(k-\kappa_0)^2\}}.$$

A *causal* representation of B_Φ is obtained by assigning to κ_0 a small positive imaginary part, which is subsequently allowed to vanish. It then follows by the usual method [20] that

$$\begin{aligned} B_\Phi &= \frac{-\mathrm{i}\kappa_0^2\Gamma B_0}{2\pi^2 c_0}\iint_{-\infty}^{\infty}\frac{l\mathrm{e}^{\mathrm{i}(kx+ly)}\,\mathrm{d}k\,\mathrm{d}l}{(l^2+k^2-\kappa_0^2)\{l^2+(k-\kappa_0)^2\}}, \\ &= \frac{\kappa_0\Gamma B_0\,\mathrm{sgn}(y)}{4\pi c_0}\int_{-\infty}^{\infty}\left[\mathrm{e}^{-|y||k-\kappa_0|} - \mathrm{e}^{\mathrm{i}|y|\sqrt{\kappa_0^2-k^2}}\right]\frac{\mathrm{e}^{\mathrm{i}kx}}{k-\kappa_0}\,\mathrm{d}k, \end{aligned} \tag{13}$$

which is equivalent to the result given by Ford and Smith [2].

The contribution from the first term in the square brackets of the integrand can be evaluated exactly, yielding $-\mathrm{i}\kappa_0 B_0\Phi(\mathbf{x})\mathrm{e}^{\mathrm{i}\kappa_0 x}/c_0$, where Φ is the potential function defined in equation (6). By setting $k=\kappa_0\cos\psi$ in the second term, we can write

$$B_\Phi = \frac{-\mathrm{i}\kappa_0 B_0\mathrm{e}^{\mathrm{i}\kappa_0 x}}{c_0}\{\Phi(\mathbf{x})+\Phi'(\mathbf{x})\}, \tag{14}$$

where

$$\Phi'(\mathbf{x}) = \frac{\mathrm{i}\Gamma \,\mathrm{sgn}(y)\mathrm{e}^{-\mathrm{i}\kappa_0 x}}{4\pi} \int_{\gamma_0} \cos(\psi/2)\mathrm{e}^{\mathrm{i}\kappa_0 r\cos(\psi-\theta)}\,\mathrm{d}\psi, \quad 0 \leqslant \theta \leqslant \pi, \tag{15}$$

is expressed in terms of the polar co-ordinates (r, θ) defined by $(x, |y|) = r(\cos\theta, \sin\theta)$. The integration contour γ_0 in the complex ψ-plane is shown in Figure 3, and consists of the three rectilinear sections $\psi = +\mathrm{i}\infty$ to $+\mathrm{i}0$, $\psi = 0$ to π, and $\psi = \pi$ to $\pi - \mathrm{i}\infty$, together with a small indentation to pass *above* the simple pole at $\psi = 0$.

To evaluate the integral in the acoustic far field ($\kappa_0 r \gg 1$) γ_0 is deformed onto the path of steepest descent γ, defined by

$$\eta = \ln[\sec(\xi - \theta) - \tan(\xi - \theta)], \quad -\frac{\pi}{2} < \xi - \theta < \frac{\pi}{2},$$

where ξ, η are the real and imaginary parts of ψ. The new path passes through the *stationary phase* point $\psi = \theta$, where it cuts the real axis at 45°. The phase $\mathrm{Re}\{\kappa_0 r\cos(\psi - \theta)\} = \kappa_0 r$ is constant on γ, and the rate of decrease in the magnitude of the exponential of the integrand is the maximum possible as ψ moves

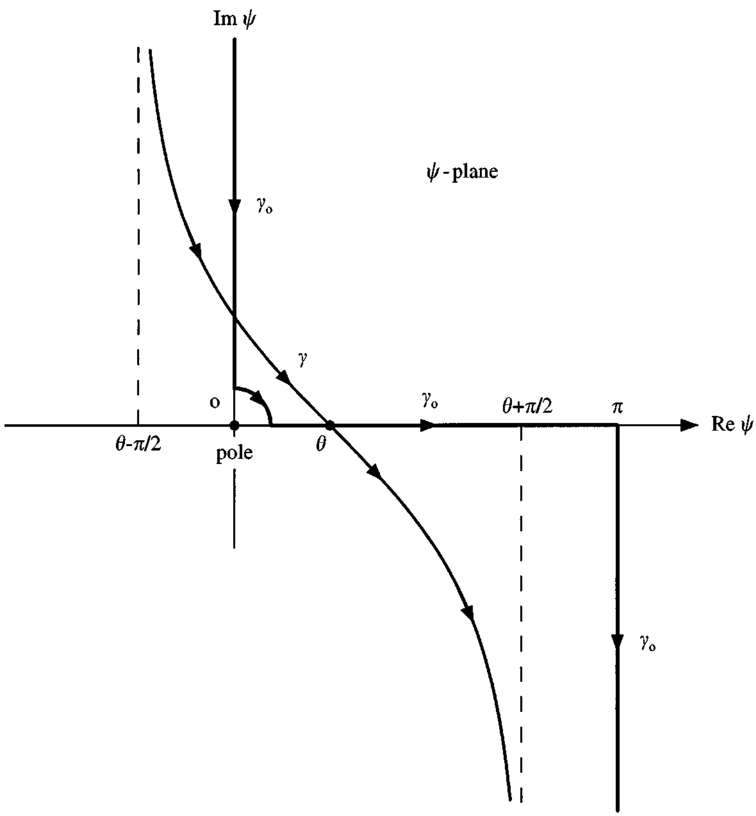

Figure 3. Integration contours in the ψ-plane.

away from $\psi = \theta$ in either direction along γ. Hence, we find

$$\Phi'(\mathbf{x}) = \frac{\mathrm{i}\Gamma\,\mathrm{sgn}(y)\mathrm{e}^{\mathrm{i}\kappa_0(r-x)}}{4\pi}\int_{\theta-\pi/2}^{\theta+\pi/2}\cos(\psi/2)\,[1-\mathrm{i}\sec(\xi-\theta)]\,\mathrm{e}^{-\kappa_0 r\sin(\xi-\theta)\tan(\xi-\theta)}\,\mathrm{d}\xi. \tag{16}$$

When $\kappa_0 r$ is large, the main contribution to the integral is from the vicinity of $\psi = \xi = \theta$. Therefore, $\sin(\xi-\theta)\tan(\xi-\theta)$ may be replaced by $(\xi-\theta)^2$ in the exponential, and the integration limits extended to $\xi - \theta = \pm\infty$. To estimate the value of the integral it is necessary to consider the two cases in which the stationary point θ is near or far from the pole at $\psi = 0$. In the first case, $\cot(\psi/2)$ $[1-\mathrm{i}\sec(\xi-\theta)]$ is replaced by $2(1-\mathrm{i})/\psi$, and the integral transformed using formulae given in reference [26] for the complex error function; in the second case it is sufficient to make the replacement $\cot(\theta/2)(1-\mathrm{i})$. We then find

$$\Phi'(\mathbf{x}) \approx \frac{\mathrm{i}\Gamma\,\mathrm{sgn}(y)}{\sqrt{2\mathrm{i}}}\left[g\left(\theta\sqrt{\frac{\kappa_0 r}{\pi}}\right) + \mathrm{i}f\left(\theta\sqrt{\frac{\kappa_0 r}{\pi}}\right)\right], \quad \theta \ll 1, \tag{17a}$$

$$\approx \Gamma\,\mathrm{sgn}(y)\cot(\theta/2)\sqrt{\frac{\mathrm{i}}{8\pi\kappa_0 r}}\,\mathrm{e}^{\mathrm{i}\kappa_0(r-x)}, \quad \theta\sqrt{\frac{\kappa_0 r}{\pi}} > O(1), \tag{17b}$$

where $g(z), f(z)$ are the Fresnel integral auxiliary functions defined in section 7.3 of reference [26]. These functions decrease smoothly from $\frac{1}{2}$ to 0 as z increases over the interval $(0, \infty)$, and satisfy

$$f(z) \sim \frac{1}{\pi z}, \quad g(z) \sim \frac{1}{\pi^2 z^3}, \quad z \to +\infty. \tag{18}$$

Equation (17(a)) and the definition (6) of Φ show that $\Phi(\mathbf{x}) + \Phi'(\mathbf{x}) = 0$ at $\theta = 0$, and this ensures that B_Φ and B are continuous across the forward scattering direction.

4. INTERPRETATION OF THE SOLUTION

According to equations (17(a) and (b)) the properties of the scattered field B_Φ are critically dependent on whether $\theta \gtrless \theta_r$, where the critical angle

$$\theta_r = \sqrt{\frac{\pi}{\kappa_0 r}}, \quad \kappa_0 r \gg 1. \tag{19}$$

The curve $\theta = \theta_r$ coincides with the parabola $x = (\kappa_0/\pi)y^2$ (plotted in Figure 2) when $\kappa_0 r \gg 1$.

A single formula for the radiation that is applicable for all radiation directions is obtained by first writing equation (14) in the form

$$B_\Phi = \frac{-\mathrm{i}\kappa_0 B_0 \mathrm{e}^{\mathrm{i}\kappa_0 x}}{c_0}\{\Phi(\mathbf{x}) + F(\theta, \theta_r)\Phi'(\mathbf{x}) + [1 - F(\theta, \theta_r)]\,\Phi'(\mathbf{x})\}. \tag{20}$$

The function $F(\theta, \theta_r)$, can be chosen arbitrarily, but we shall assume that $F(\theta, \theta_r) = 1$ for $0 < \theta \leqslant \theta_r$, and that $F(\theta, \theta_r)$ decreases monotonically and rapidly to zero for

$\theta > \theta_r$. The second term in the brace brackets is therefore substantially different from zero only within the parabola $x = (\kappa_0/\pi)y^2$, where $\Phi'(\mathbf{x})$ may be approximated by equation (17a). The final term in the brace brackets is non-zero only outside the parabola, where equation (17b) can be used to approximate $\Phi'(\mathbf{x})$.

Combining this with the dipole scattered field (12) and with the incident plane wave (3), we have

$$B = B_1 + B_2, \tag{21}$$

where, with the shorthand notation $F = F(\theta, \theta_r)$, $f = f(\theta/\theta_r)$, $g = g(\theta/\theta_r)$,

$$\begin{aligned} B_1 &= B_0 \mathrm{e}^{\mathrm{i}\kappa_0 x}\left\{1 - \frac{\mathrm{i}\kappa_0}{c_0}\left(\Phi(\mathbf{x}) + \frac{\Gamma \operatorname{sgn}(y)}{\sqrt{2\mathrm{i}}} F(g + \mathrm{i}f)\right)\right\} \\ &\approx B_0 \exp\left\{\mathrm{i}\kappa_0\left[x - \frac{1}{c_0}\left(\Phi(\mathbf{x}) + \frac{\Gamma \operatorname{sgn}(y)}{\sqrt{2\mathrm{i}}} F(g + \mathrm{i}f)\right)\right]\right\}, \end{aligned} \tag{22}$$

$$B_2 \approx \frac{-\kappa_0 \Gamma B_0 \operatorname{sgn}(y) \mathrm{e}^{\mathrm{i}\kappa_0 r}}{c_0\sqrt{8\pi \mathrm{i}\kappa_0 r}}\{\sin\theta - (1 - F)\cos(\theta/2)\}. \tag{23}$$

The component B_1 describes a slowing evolving incident wave propagating across the vortex flow, and is the corrected form of the zeroth order approximation (9) of section 3.1. It represents a motion that is continuous everywhere in the fluid away from the vortex core, including along the forward scatter ray $x > 0$, $y = 0$. The second component B_2 is a cylindrically spreading disturbance that represents waves decaying like $1/\sqrt{\kappa_0 r}$ with distance r from the vortex.

The distortion of the wave crests of the incident sound by the mean flow may now be determined. From equation (22), it is seen that the corrected form of equation (10) for the curvilinear wave crests is

$$\frac{x}{\lambda} + \frac{\varepsilon}{4\pi}\operatorname{sgn}(y)\left(H(x) - \frac{\operatorname{sgn}(x)}{\pi}\arctan\left|\frac{y}{x}\right| - F(g + f)\right) = n, \quad n = 0, \pm 1, \pm 2, \ldots, \tag{24}$$

The functions f, g can be evaluated in the range $0 \leqslant x < \infty$ from rational approximations given in reference [26], section 7.3.

Figure 4 illustrates the wave crests defined by equation (24) for the case considered in section 3.1 of $\varepsilon = \pi$, when F is taken to be

$$F(\theta, \theta_r) = \begin{cases} 1, & 0 \leqslant \theta < \theta_r, \\ \exp[-(\theta/\theta_r - 1)^2], & \theta \geqslant \theta_r. \end{cases} \tag{25}$$

Outside the parabola $x = (\kappa_0/\pi)y^2$ the wave crests are identical with the "phase shifted" crests plotted in Figure 2 from the zeroth order approximation. Within the parabola the correction $F(g + f)$ in equation (24), to the zeroth order phase of the approximation (9), produces a smooth transition between crests on opposite sides of the forward scatter ray. The scattered field vanishes in both the forward and back directions ($\theta = 0, \pi$), but the *slope* of the wavefront is maximal in the direction of forward scatter. By making use of the asymptotic formulae (18), it can be shown

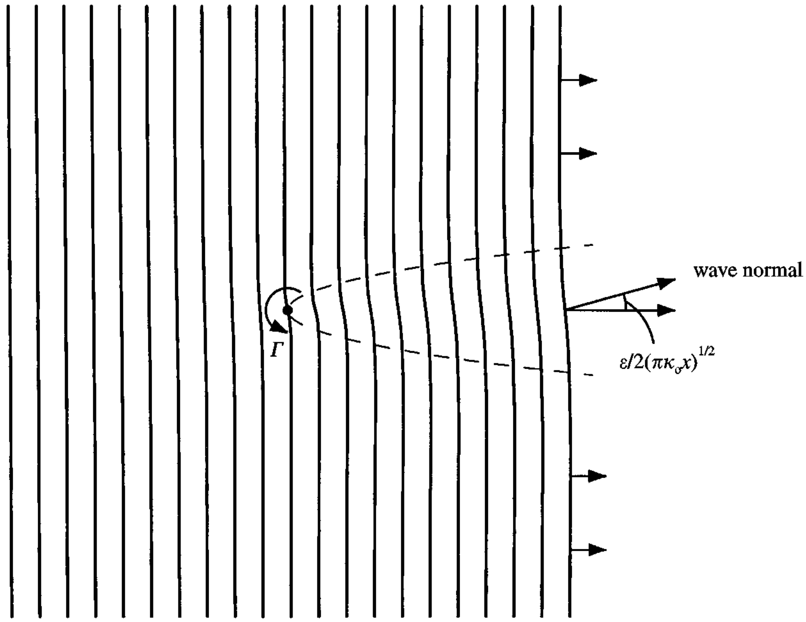

Figure 4. Wave crests defined by the Born approximation (24) when $\varepsilon = \pi$.

that the wave normal is maximally inclined at an angle $\sim \varepsilon/2\sqrt{\pi\kappa_0 x}$ to the incident wave normal (the x-axis) at large distances from the vortex in the forward scattering direction. Ultimately, the wave crests within the parabolic domain relax back to their undisturbed form, i.e., become parallel to the incident wave crests.

After traversing the vortex the wave fronts become concave in the upper region ($x > 0,\ y > 0$) and convex in the lower region ($x > 0,\ y < 0$). Focusing and defocusing of incident wave energy must therefore make the wave amplitude in these regions, respectively, larger and smaller than that of the incident wave. This is illustrated in Figure 5, which depicts plots of

$$\frac{|B_1|}{|B_0|} \approx \exp\left(\frac{\varepsilon\,\mathrm{sgn}(y)}{2} F(f-g)\right),$$

as a function of y for $x = \lambda, 2\lambda, \ldots, 10\lambda$, where $\lambda = 2\pi/\kappa_0$ is the wavelength of the incident wave. Because $f(\theta/\theta_r) - g(\theta/\theta_r)$ is positive for $\theta > 0$, and attains an absolute maximum value $\sim$0·23 at $\theta \approx \frac{2}{3}\theta_r$, the energy maxima and minima occur on the parabola

$$x \approx \frac{9\kappa_0 y^2}{4\pi},$$

which lies within the critical parabola $\theta = \theta_r$ plotted as the broken-line curve in the figure.

The transmitted incident wave is well approximated by the zeroth order approximation (9) outside the critical parabola. However, there are also cylindrically spreading “scattered” waves defined by B_2 of equation (23), which are

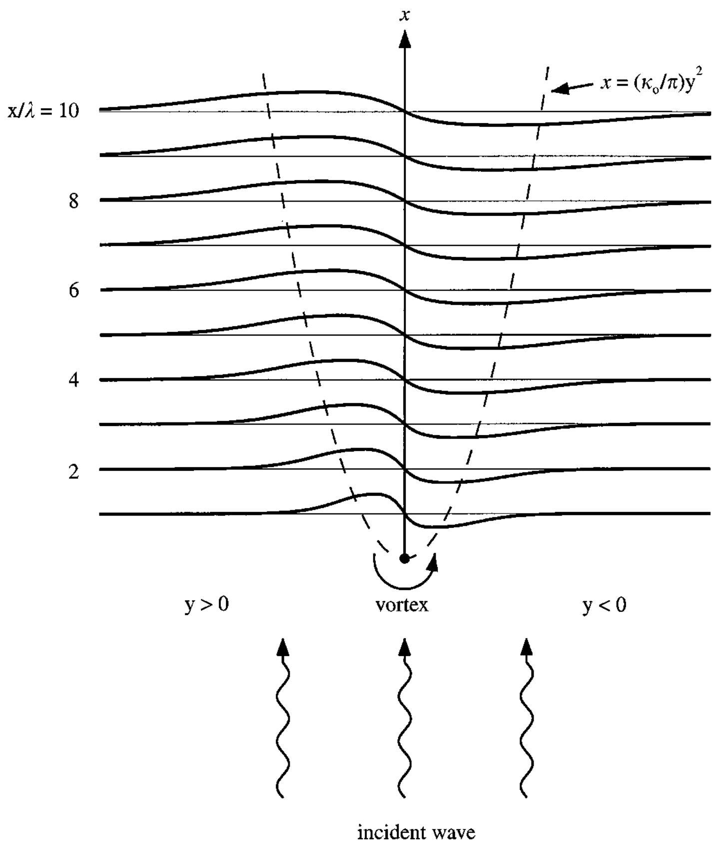

Figure 5. Relaxation of wave amplitude after interaction with the vortex.

of the type normally associated with scattering from a localized disturbance. Because of the increasing width of the parabola as $x \to +\infty$ (like $\sqrt{\lambda x}$), within which a progressively increasing section of the perturbed incident wavefront relaxes to its undisturbed form, the directivity $|B_2/B_0|$ of the scattered waves varies with distance r/λ, as illustrated in Figure 6. The two symmetric radiation peaks in the forward direction always lie outside the critical parabola (see Figure 7) at $\theta \approx 2{\cdot}4\theta_r$, where $|B_2/B_0| \sim 0{\cdot}08\varepsilon$ (although it must be remembered that the precise values of these estimates are dependent on the choice of the transition function $F(\theta, \theta_r)$), and therefore increase in magnitude relative to the sound scattered in other directions as $r/\lambda \to \infty$, and, in particular, relative to the two backscatter lobes which peak in directions $\sim \pm 52°$ from the negative x-axis. The large forward scattered lobes account for energy released during the relaxation of the refracted transmitted wave.

5. CONCLUSION

The two-dimensional interaction of a plane, time-harmonic sound wave and the low Mach number flow induced by a rectilinear vortex of small core diameter are

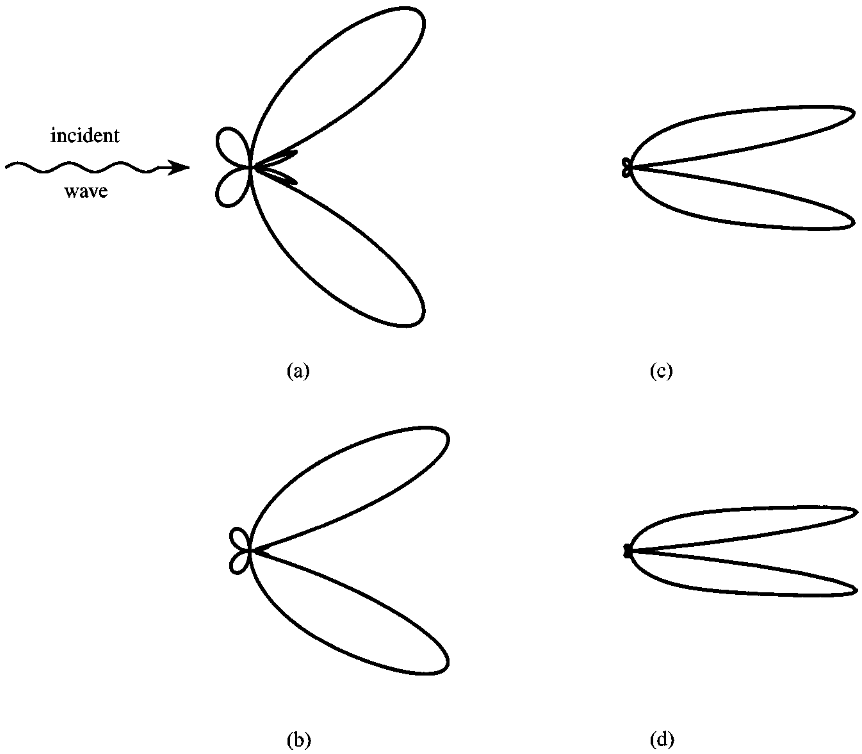

Figure 6. Dependence on radial distance r/λ of the linear directivity $|B_2/B_0|$ of the cylindrically spreading sound; each plot is normalized with respect to peak value: (a) $r/\lambda = 5$, (b) 10, (c) 50, (d) 100.

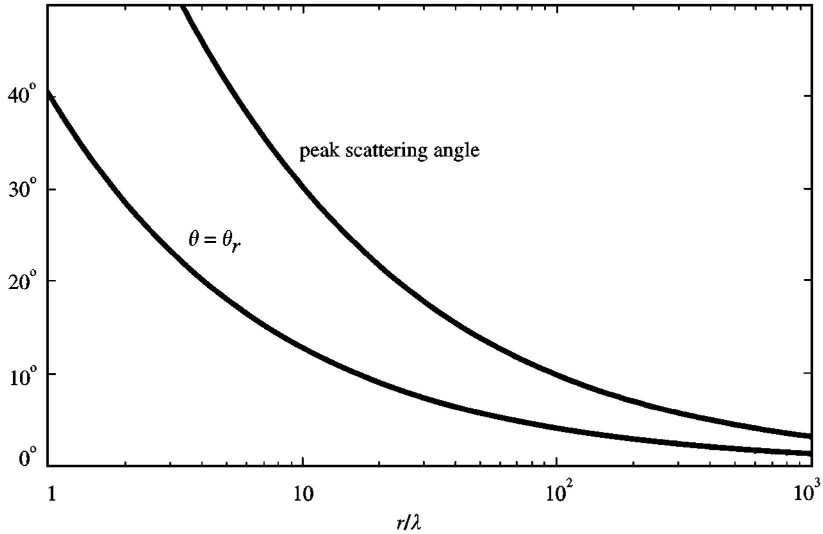

Figure 7. Peak scattering angle for the cylindrically spreading wave B_2.

dominated by a smooth distortion of the wave crests of the incident wave on passing across the core and their ultimate relaxation to their undisturbed forms. In the Born approximation, the scattered field has nulls in the forward and back scattering directions, but the interaction of the incident wave with non-acoustically compact components of the vortex velocity field causes wavefront distortion, and the phase of the incident wave to undergo a significant variation across the region bounded by the parabola $x = (\kappa_0/\pi)y^2$, whose axis extends along the forward scattering direction. Within this region the wave crests are concave and convex, respectively, on opposite sides of the axis of the parabola, and focusing and defocusing of wave energy leads to corresponding increases and decreases in wave amplitude. The curvature of the wave fronts decreases like $\sqrt{\lambda/x}$ with increasing axial distance x from the vortex core, so that the wave amplitude and phase return asymptotically to the respective values they would have attained in the absence of the vortex.

Cylindrically spreading waves, whose amplitudes are $\sim\sqrt{\lambda/r}$, are scattered into the region outside the parabola. The directivity is symmetric with respect to the incident wave direction of propagation, and is characterized by two large lobes close to the direction of forward scattering, and two smaller lobes in directions $\sim \pm 52^\circ$ to the backscatter direction. These waves can be attributed to three sources: (1) the transverse acoustic dipole associated with the back-and-forth translational oscillations of the vortex core at the acoustic particle velocity of the incident wave, (2) interaction of the incident wave with acoustically compact components of the potential flow velocity of the vortex, and (3) the steady release of energy by the relaxing refracted transmitted wave.

ACKNOWLEDGMENTS

The author expresses his gratitude to Dr Rupert Ford for making available an advance copy of Ford and Smith [2].

REFERENCES

1. P. V. Sakov 1993 *Acoustical Physics* **39**, 280–282. Sound scattering by a vortex filament.
2. R. Ford and S. G. L. Smith 1999 *Journal of Fluid Mechanics* **386**, 305–328. Scattering of acoustic waves by a vortex.
3. S. O'Shea 1975 *Journal of Sound and Vibration* **43**, 109–116. Sound scattering by a potential vortex.
4. M. S. Howe 1975 *Journal of Fluid Mechanics* **71**, 625–673. Contributions to the theory of aerodynamic sound, with application to excess jet noise and the theory of the flute.
5. A. L. Fabrikant 1983 *Soviet Physics Acoustics* **29**, 152–155. Sound scattering by vortex flows.
6. T. Colonius, S. K. Lele and P. Moin 1994 *Journal of Fluid Mechanics* **260**, 271–298. The scattering of sound waves by a compressible vortex—numerical simulations and analytical solutions.
7. R. Berthet and F. Lund 1995 *Physics of Fluids* **7**, 2522–2524. The forward scattering of sound by vorticity.
8. S. M. Candel 1979 *Journal of Fluid Mechanics* **90**, 465–507. Numerical solution of wave scattering problems in the parabolic approximation.
9. J. Reinschke, W. Mohring and F. Obermeier 1997 *Journal of Fluid Mechanics* **333**, 273–300. Scattering of sound waves by a cylindrical vortex: a semi-analytical theory.

10. M. A. Hollingsworth and E. J. Richards 1995 *Aeronautical Research Council Report No.* 17985, *Fluid Motion Subcommitte* 2323, *London*. A schlieren study of the interaction of a vortex and a shock wave.
11. D. S. Dosanjh and T. M. Weeks 1965 *American Institute of Aeronautics and Astronautics Journal* **3**, 216–223. Interaction of a starting vortex as well as a vortex street with a traveling shock wave.
12. W. C. Horne 1983 *American Institute of Aeronautics and Astronautics Paper* 83-0676. Measurements of the scattering of sound by a line vortex.
13. T. Kambe and U. Mya Oo 1981 *Journal of the Physical Society of Japan* **50**, 3507–3516. Scattering of sound by a vortex ring.
14. K. Tanaka and S. Ishii 1981 *Journal of the Physical Society of Japan* **51**, 1992–1999. Scattering of a plane sound wave by a vortex pair.
15. T. Kambe 1982 *Journal of the Japanese Society of Fluid Mechanics* **1**, 149–165. Scattering of sound by vortex systems (in Japanese).
16. M. S. Howe 1983 *Journal of Sound and Vibration* **87**, 567–571. On the scattering of sound by a vortex ring.
17. V. F. Kopiev and E. A. Leontiev 1987 *Fluid Dynamics* **22**, 398–409. Radiation and scattering of sound from a vortex ring.
18. R. H. Kraichan 1953 *Journal of the Acoustical Society of America* **25**, 1096–1104. The scattering of sound in a turbulent medium.
19. M. J. Lighthill 1953 *Proceedings of the Cambridge Philosophical Society* **49**, 531–551. On the energy scattered from the interaction of turbulence with sound or shock waves.
20. M. S. Howe 1998 *Aoustics of Fluid–Structure Interaction*. Cambridge: Cambridge University Press.
21. R. B. Lindsay 1948 *Journal of the Acoustical Society of America* **20**, 89–94. Compressional wave front propagation through a simple vortex.
22. T. M. Georges 1971 *Journal of the Acoustical Society of America* **51**, 206–209. Acoustic ray paths through a model vortex with a viscous core.
23. E. G. Broadbent 1977 *Journal of the Institute of Mathematics and its Applications* **19**, 1–27. Acoustic ray theory applied to vortex refraction.
24. H. Lamb 1932 *Hydrodynamics*. Cambridge: Cambridge University Press, sixth edition, reprinted 1993.
25. K. Taylor 1978 *Proceedings of the Royal Society of London* **A 363**, 271–281. A transformation of the acoustic equation with implications for wind tunnel and low speed flight tests.
26. A. Abramowitz and I. A. Stegun 1972 (editors) *Handbook of Mathematical Functions* (Tenth corrected printing), United States Department of Commerce, National Bureau of Standards, Applied Mathematics Series No. 55.